Vol. 04, Iss. 3 (2026) 1-14, DOI: 10.61552/JME.2026.03.002

JME

Journal of Materials and Engineering

www.jme.aspur.rs

Effects of Nitrogen Content on Square Wave Anodic Stripping Voltammetric Performance of Nitrogen-Doped Tetrahedral Amorphous Carbon Thin Films

Nay Win Khun[a,b,*], Koh Chin Chong[a], Adrian Wei-Yee Tan[c], Erjia Liu[a]

[a]*School of Mechanical and Aerospace Engineering, Nanyang Technological University, 50 Nanyang Avenue, Singapore 639798, Singapore,*
[b]*Institute of Microelectronics and Optoelectronics, Faculty of Electronics and Information Technology, Warsaw University of Technology, Koszykowa 75, 00-662 Warszawa, Poland,*
[c]*Smart Manufacturing and Systems Research Group (SMSRG), University of Southampton Malaysia, Iskandar Puteri 79100, Johor, Malaysia.*

Keywords:

N-taC thin films
N doping
LSCV
SWASV
Pb^{2+} and Cu^{2+} ions

* Corresponding author:

Nay Win Khun
E-mail: khunnaywin@gmail.com

Received: 21 December 2024
Revised: 1 March 2025
Accepted: 11 April 2025

A B S T R A C T

Nitrogen-doped tetrahedral amorphous carbon (N-taC) thin films were prepared on silicon (Si) substrates via filtered cathodic vacuum arc (FCVA) deposition by varying the N_2 flow rate from 10 to 60 sccm to get different N contents in the films. The electrochemical potential windows (EPWs) of the N-taC thin films were measured in potassium chloride (KCl) solution by applying a linear sweep cyclic voltammetric (LSCV) technique. The square wave anodic stripping voltammograms (SWASVs) of lead (Pb) and copper (Cu) on the film surfaces were acquired by varying deposition time and potential and metal ion concentration. The effects of N content on the EPWs and SWASV performance of the N-taC thin films were also investigated. The results clearly showed the apparent influences of deposition time and potential, metal ion concentration, and N content on the SWASVs of both Pb and Cu obtained by the N-taC thin films. It was found that the N-taC thin films were able to detect Pb^{2+} and Cu^{2+} ions in the KCl solution at the µM level.

1. INTRODUCTION

The presence of heavy metals such as mercury (Hg), lead (Pb), copper (Cu), etc., released from anthropogenic sources, in the aquatic ecosystem implicates not only biota but also human beings [1-3]. Water may be seen as clean and transparent as it is, but there are usually those heavy metals present in it that are not visible to the human eye. When water containing undetected heavy metals is consumed, they can have harmful and

detrimental effects on the human body since most of them are toxic [4]. An accumulation of heavy metals in the body can eventually lead to serious health problems over time.

Pb is one of the most toxic heavy metals with a wide range of applications, such as batteries, printing, pipes, pigments, fuels, welding, and so on [1-3,5]. The Pb concentration of more than 4×10^{-6} M in drinking water is detrimental to fetuses and children with possible development of neurological problems [1-3,5]. For instance, an overdose of Pb results in poisoning, which can cause irreversible neurological damage, renal disease, cardiovascular effects, hypertension, and reproductive toxicity [1-3,5]. Although Cu has relatively low toxicity to human beings and its small concentrations are essential to life, prolonged consumption of excessive Cu of more than 8×10^{-5} M can result in some health complications with adverse chronic effects (e.g., liver failure) [1-3,6]. Cu can come from many sources, such as waste from metal cleaning and plating baths, the fertilizer industry, paperboard, paper, pulp, and so on [1-3,6]. The use of contaminated drinking water with heavy metals can cause their accumulation in the bodies of human beings and animals, leading to serious health problems [7]. Therefore, it is of paramount importance that the drinking water is free of heavy metals before consumption. One possible way to ensure that the water is clean and hygienic for domestic use is to detect the presence of any unwanted heavy metals in it at an early stage and remove them effectively [8]. Therefore, it becomes challenging for analysts to quickly detect and effectively determine heavy metals in aqueous solutions.

Hg and carbon (C) (glassy carbon, graphite, etc.)-based electrodes are widely used for electroanalytical purposes, but they have their own limited electrochemical performance [9-11]. Boron (B)-doped diamond thin films have been introduced for stripping analysis of various heavy metals such as Pb, Cu, cadmium (Cd), zinc (Zn), manganese (Mn), silver (Ag), etc. at μM level [12-14]. But they require high deposition temperatures, which demand high energy consumption and manufacturing costs [12-14]. Compared to B-doped diamond thin films, diamond-like carbon (DLC) thin films can be practically prepared at room temperature (RT) [9,15-18]. In addition, DLC thin films are well known for their exceptional properties, such as high hardness, low coefficient of friction, and excellent wear resistance [19,20]. Besides, the insulating property of DLC thin films causes them to be excellent in corrosion resistance in aggressive solutions but makes them impossible to be applied in electrochemical applications [19-21]. However, nitrogen (N) doping can make DLC thin films conductive to be suitable for electrochemical analysis [9,15-18]. Yoo et al. [15] first reported that N doping improved the electrical conductivity of DLC thin films and made them suitable for electrochemical applications. The N-DLC thin films had a wider electrochemical potential window (EPW) in an HClO4 solution than B-doped diamond thin films. Zeng et al. [22,23] introduced N-DLC thin films for stripping analysis of Pb^{2+}, Cd^{2+}, and Cu^{2+} ions in an aqueous solution and measured their EPWs in various aqueous solutions. Lagrini et al. [24] studied the EPWs of N-DLC thin films in a $LiClO_4$ solution with different N_2 partial pressures. Khun et al. [16,25] further reported the EPWs of N-DLC thin films in various aqueous solutions and their electrochemical performance of detecting single and multiple elements in an aqueous solution. Based on the reported results in the literature, it is still necessary to further improve the sensitivity of N-DLC thin films to heavy metal ions by reducing their background currents for their successful application in electrochemical analysis.

The filtered cathodic vacuum arc (FCVA) deposition method is often chosen to produce taC thin films over other physical vapor deposition (PVD) methods for electrochemical applications because of several advantages, such as the high percentage of sp^3 bonds, uniform thickness, good film quality, high deposition rate, and relatively low operating cost [26]. As a result, the taC thin films have higher hardness, Young's modulus, wear, and corrosion resistance compared to sputtered DLC thin films. It is therefore expected that taC thin films have high resistance to prompt anodic dissolution in electrolytes, which is essential for promising thin film electrodes, since the poor corrosion resistance of an electrode can negatively affect its electrochemical performance, such as sensitivity, accuracy, repeatability, robustness, stability, etc. [27].

Voltammetry is an analytical technique based on the measure of the current flowing through an electrode that is immersed in an electrolyte containing electrochemically active species while a potential scan is imposed on it [9]. The cyclic voltammetric (CV) technique is always used to first

access the electrochemical performance of new electrodes by measuring their EPWs in various aqueous solutions because of its high information content and simplicity [9]. An EPW is defined by a difference in potentials for hydrogen (H_2) and oxygen (O_2) gas evolution, within which metals are supposed to be detected, so that the wider EPW allows the detection of a greater variety of metals in aqueous solutions [9,23,25,28,29]. The stripping voltammetric (SV) technique offers a simple, fast, and cheap way of detecting heavy metals among many electroanalytical techniques [9]. Although there are several SV techniques, such as anodic, cathodic, and absorptive SV techniques, the anodic stripping voltammetric (ASV) technique is the most broadly used technique for heavy metal detection because of its remarkably high sensitivity to metal ions, very low detection limit, and ability to simultaneously detect multiple heavy metals by relatively inexpensive instrumentation [9,23,25,28,29]. The ASV technique consists of two main steps: a pre-concentration or accumulation step, in which analytes of interest are accumulated from the solution onto a suitable working electrode surface by applying a negative deposition potential, and a stripping step involving pre-concentrated analytes that are then stripped from the electrode surface into the solution by the application of a potential scan, with a resulting Faradaic current allowing direct quantification of the number of analytes present [9,23,25,28,29]. The stripping voltammograms of heavy metals are greatly influenced by their concentrations as well as electrochemical deposition parameters such as deposition time and potential [9,23,25,28,29]. It is therefore necessary to systematically investigate the effects of metal ion concentrations and deposition parameters on the ASV performance of N-taC thin films.

In this study, N-taC thin films were prepared on Si substrates via FCVA deposition by varying the N_2 flow rate from 10 to 60 sccm. The effects of N content on their EPWs in an aqueous KCl solution were evaluated using the linear sweep cyclic voltammetric (LSCV) technique. Their detection performance of Pb^{2+} and Cu^{2+} ions was systematically investigated using the square wave anodic stripping voltammetric (SWASV) technique with respect to N content, deposition time and potential, and metal ion concentration, since the SWASV technique had excellent sensitivity, rejection of background current, and fast scanning speed [9].

2. EXPERIMENTAL DETAILS

2.1 Sample preparation

A FCVA deposition system (Nanofilms) was used to deposit N-taC thin films with an estimated thickness of 100 nm on Si substrates (100, n-type, 150 mm diameter, 0.7 mm thick, 0.001-0.0035 Ωcm). For the N dopant, the N_2 gas was introduced into the deposition chamber via a mass flow controller at flow rates of 10, 20, 40, and 60 sccm, while a pure graphite target (99.995%) was used as the C source. All the depositions were carried out for 250 s at RT (~22-24˚C), with a fixed substrate pulsed bias of 800 V and a current of 30 A on the cathode. Prior to the film deposition, the Si substrates were cleaned with an N_2 ionizing gun. It was found that the N contents of the N-taC thin films measured by X-ray photoelectron spectroscopy (XPS, Kratos) with monochromatic Al Kα (1486.6 eV) X-ray radiation were 2.6, 2.8, 3.4, and 5.1 at.% for 10, 20, 40, and 60 sccm N_2, respectively.

2.2 Characterization

All the electrochemical measurements were carried out using a BioNano LK6200 electrochemical workstation. A K0235 flat cell kit with three electrodes was used. A platinum mesh was used as the counter electrode, while a standard silver/silver chloride (Ag/AgCl) electrode in a saturated KCl solution (0.197 V at 25˚C) was used as the reference electrode. The N-taC thin film-coated samples with 2 cm × 2 cm were used as the working electrodes, and their back sides were coated with a gold layer to make them have a good electrical connection. The testing areas of the working electrodes were a circle of 1 cm in diameter. The amount of different solutions used was 250 ml.

The EPWs of the N-taC thin films in a deaerated and unstirred 0.1 M KCl solution without adjusting its pH value were measured using the LSCV technique by scanning from -2 V to 3 V at a scan rate of 100 mV/s.

The ASV performance of the N-taC thin films in a deaerated and unstirred 0.1 M KCl solution was analyzed using the SWASV technique. Both the potential increase and amplitude were 0.15 V. The frequency was 10 Hz, and the quiet time was 10 s. These parameters were fixed to measure the

stripping currents of both Pb and Cu with respect to deposition time and potential and metal ion concentration. The deposition potential of -1.2 V was fixed to get the SWASVs of both Pb and Cu with different deposition times of 60 s to 240 s. The deposition time of 60 s was fixed for the SWASVs of both Pb and Cu with different deposition potentials of -0.8 to -1.2 V. The deposition potential of -1.2 V and the deposition time of 60 s were fixed for the SWASVs of both Pb and Cu with different metal ion concentrations of 1×10^{-6} M to 1.5×10^{-5} M.

3. RESULTS AND DISCUSSION

3.1 Effect of N_2 flow rate on LSCVs of N-taC thin films

Figure 1 shows the LSCVs of the N-taC thin films with different N_2 flow rates measured in a 0.1 M KCl solution. In a CV, a potential difference between hydrogen ($2H^+ + 2e^- \rightarrow H_2\uparrow$) and oxygen ($4OH^- \rightarrow 2H_2O + 4e^- + O_2\uparrow$) gas evolution gives rise to an EPW where decomposition of water occurs ($H_2O \rightarrow H^+ + OH^-$) [9,23,25,28,29]. The wider EPW allows detection of a wider range of different elements in aqueous solutions for metal tracing analysis, since specific metal elements within the EPW can only be detected [9,23,25,28,29]. The N-taC thin film with a N_2 flow rate of 10 sccm has potentials of -1.5 V and 2.3 V for H_2 and O_2 gas evolution, respectively, on its surface, so it has a wide EPW of 3.8 V, as found in Figure 1 and Table 1. Increasing the N_2 flow rate to 60 sccm shifts the potentials for H_2 and O_2 gas evolution on the N-taC thin film surface to -1.1 V and 2 V, respectively, as well as decreases its EPW to 3.1 V. The increased N content of the N-taC thin film decreases its electrical resistivity because the extra electron of the doped N atom enhances its n-type semi-conductivity, while the N doping narrows its band gap via its graphitization [28,29]. The lower electrical resistivity of the N-taC thin film with a higher N_2 flow rate results in an earlier evolution of H_2 and O_2 gases via the higher kinetics of electron transfer through it, which is confirmed by the shifts of potentials for H_2 and O_2 gas evolution to less negative and positive potentials, respectively, as found in Table 1 [22,23,25]. The increased N content of the N-taC thin film, therefore, decreases its EPW, which means that a range of different elements for metal tracing analysis is decreased as a result of an earlier occurrence of the obstacle associated with H_2 and O_2 gas evolution during electrochemical measurements.

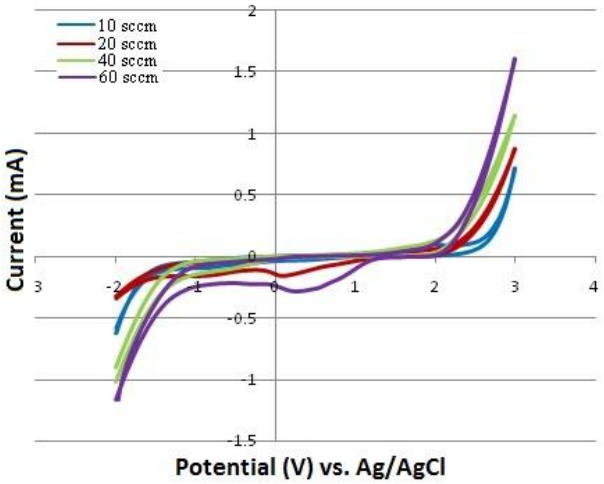

Fig. 1. LSCVs of N-taC thin films with different N_2 flow rates measured in a 0.1 M KCl solution at a scan rate of 100 mV/s.

Table 1. EPWs of N-taC thin films with different N_2 flow rates

N_2 flow rate	$H_2\uparrow$	$O_2\uparrow$	EPW
10 sccm	-1.5 V	2.3 V	3.8 V
20 sccm	-1.4 V	2.2 V	3.6 V
40 sccm	-1.2 V	2.1 V	3.3 V
60 sccm	-1.1 V	2.0 V	3.1 V

The positive portions of the EPWs of the N-taC thin films are wider than their negative ones for all the N_2 flow rates, which implies that they can trace more elements with positive electrochemical potentials. Although the EPWs of the N-taC thin films decrease with increased N content, their positive portions are still wider than their negative ones, as reported in Table 1. The peak observed in the reduction half-cycle probably results from the catalytic activity for Cl_2/Cl^- [15,23,25]. No observation of any peak in the oxidation half-cycle indicates the durability of the N-taC thin film to high anodic potentials in the KCl solution [23]. The slight slope of current versus potential in the oxidation half-cycle is indicative of a contribution of background current, which may result from the increased anodic dissolution of surface oxides of the N-taC thin film, exposed to

air for some time after the deposition, with shifting the applied potential to more positive values [25]. Nevertheless, the contribution of background current to the LSCVs of the N-taC thin films is not very significant for all the N_2 flow rates, which is essential to their high signal-to-background ratios and high sensitivity to heavy metal ions [9,25].

3.2 Effect of deposition time on SWASVs of Pb and Cu

Figures 2a-d show the SWASVs of Pb obtained by the N-taC thin films with different N_2 flow rates, measured in a 1×10^{-6} M Pb^{2+} + 0.1 M KCl solution at a deposition potential of -1.2 V, as a function of deposition time.

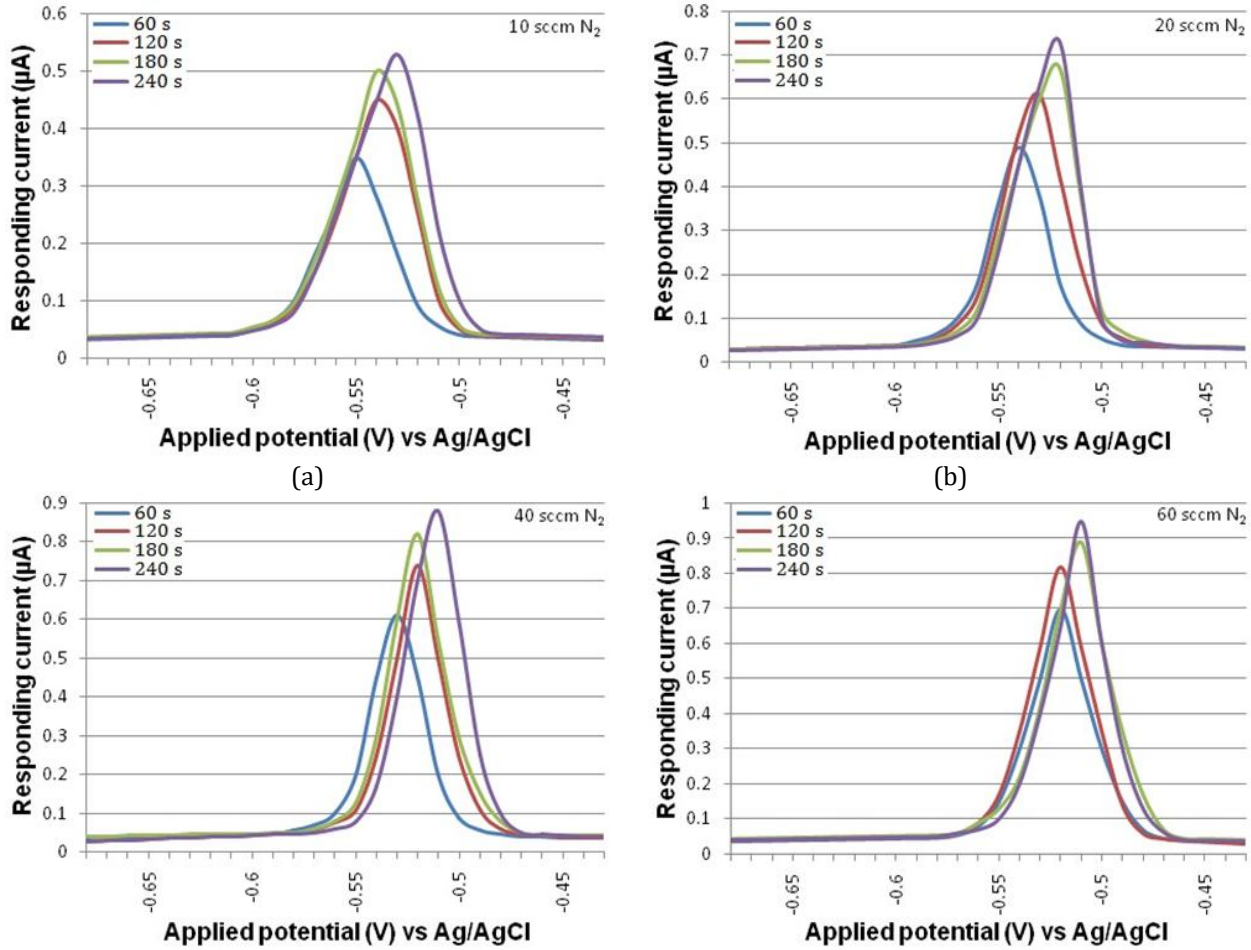

Fig. 2. SWASVs of Pb obtained by N-taC thin films with N_2 flow rates of (a) 10 sccm, (b) 20 sccm, (c) 40 sccm, and (d) 60 sccm in a 1×10^{-6} M Pb^{2+} + 0.1 M KCl solution as a function of deposition time. The deposition potential was -1.2 V.

Generally, there are two main steps for the AS analysis of Pb: (1) pre-concentration of Pb^{2+} ions and (2) stripping of reduced Pb atoms. In the pre-concentration step, Pb^{2+} ions in the KCl solution are reduced into Pb atoms on the N-taC thin film surface via a reduction reaction of $Pb^{2+} + 2e^- \rightarrow Pb$ at an applied negative potential. Then, in the stripping step, the reduced Pb atoms on the N-taC thin film surface are stripped into Pb^{2+} ions into the solution through an oxidation reaction of $Pb \rightarrow Pb^{2+} + 2e^-$ by shifting an applied potential to more positive values with the generation of a Faradaic current [12,16]. Since the amount of reduced Pb atoms on the N-taC thin film surface depends on the deposition time, an increase in the deposition time results in an increase in the amount of reduced Pb atoms on the film surface in the pre-concentration step and, subsequently, a proportional increase in the amount of stripped Pb^{2+} ions in the stripping step [12,16]. Therefore, the stripping peak intensities of Pb obtained by the N-taC thin films apparently increase with increased deposition time for all the N_2 flow rates, as shown in Figures 2a-d.

It has been known that the increased N content in the N-taC thin film decreases its electrical resistivity, which in turn increases the kinetics of electron transfer through it to the film/solution interface [16,28,29]. Therefore, the higher kinetics of electron transfer facilitates the reaction of the N-taC thin film to give rise to a larger amount of reduced Pb atoms on its surface within the same amount of deposition time, resulting in a proportionally larger amount of stripped Pb^{2+} ions [9,16-18]. Therefore, the promoted reaction of the N-taC thin film is responsible for an increase in the stripping peak intensity of Pb with an increased N_2 flow rate for the same deposition time, as shown in Figures 2a-d.

In Figures 2a-d, the stripping potentials of Pb obtained by the N-taC thin films with different N_2 flow rates shift to less negative values with longer deposition times. As reported above, the longer deposition time is responsible for the larger amount of stripped Pb^{2+} ions. According to the Nernst Equation [9,16]:

$$E = E^o + \frac{RT}{zF} \ln [Pb^{2+}] \quad (1)$$

where E = stripping potential, E^o = standard half-cell potential of Pb, R = universal gas constant, T = absolute temperature in Kelvin, z = number of electrons transferred in the half-reaction, and F = Faraday constant, it is found that the E value becomes less negative with a higher concentration of stripped Pb^{2+} ions. This causes the stripping potential (E) of Pb to shift to a less negative value with a longer deposition time. The SWASVs of Pb obtained for different deposition times also shift to less negative values with higher N_2 flow rates in Figures 2a-d. From the point of Pb^{2+} ion concentration, this can be explained by the less negative value of the E with the higher concentration of stripped Pb^{2+} ions associated with the promoted electrical conductivity of the N-taC thin film [9,16-18]. Figures 3a-d show the SWASVs of Cu obtained by the N-taC thin films with different N_2 flow rates, , measured in a 1×10^{-6} M Cu^{2+} + 0.1 M KCl solution at a deposition potential of -1.2 V, as a function of deposition time. The stripping peak intensities of Cu become higher with a longer deposition time for all the N_2 flow rates. It indicates that increasing the deposition time increases the amount of reduced Cu atoms on the film surface via a reduction reaction of $Cu^{2+} + 2e^- \rightarrow Cu$ in the pre-concentration step and then results in a proportional increase in the amount of stripped Cu^{2+} ions via an oxidation reaction of $Cu \rightarrow Cu^{2+} + 2e^-$ in the stripping step [9,30,31]. It is consistently found that the stripping peak intensities of Cu obtained for different deposition times are higher for the higher N_2 flow rates as a result of the promoted electrical conductivity of the N-taC thin film.

In Figures 2a-d and 3a-d, the well-defined stripping peaks of both Pb and Cu are obtained by the N-taC thin film with the lowest N_2 flow rate of 10 sccm for the shortest deposition time of 60 s in the KCl solution with 1×10^{-6} M Pb^{2+}. It indicates that the N-taC thin film, even with the lowest N content of 2.7 at.%, can effectively trace Pb^{2+} and Cu^{2+} ions at μM level.

In Figures 3a-d, the stripping potentials of Cu shift to less negative values with longer deposition times for all the N_2 flow rates, which can be related to the larger amount of stripped Cu^{2+} ions according to the Nernst Equation [9,16]. Besides, the stripping potentials of Cu obtained by the N-taC thin films with higher N_2 flow rates exist at less negative values compared to those obtained by the ones with lower N_2 flow rates as a result of the larger amount of stripped Cu^{2+} ions [9,16,18].

It is clear that the stripping potentials of both Pb and Cu are influenced by the deposition time and the N_2 flow rate. In addition, the stripping potentials of Cu exist at less negative values than those of Pb, as shown by the comparison of Figures 2a-d and 3a-d, and such a difference in their stripping potentials is due to their different redox potentials [16].

Figure 4 shows the replotted stripping peak currents of Pb and Cu as a function of deposition time. The stripping peak currents of both Pb and Cu become higher with longer deposition times for all the N_2 flow rates, confirming that the longer deposition time gives rise to more reduction of both Pb^{2+} and Cu^{2+} ions on the N-taC thin film surface.

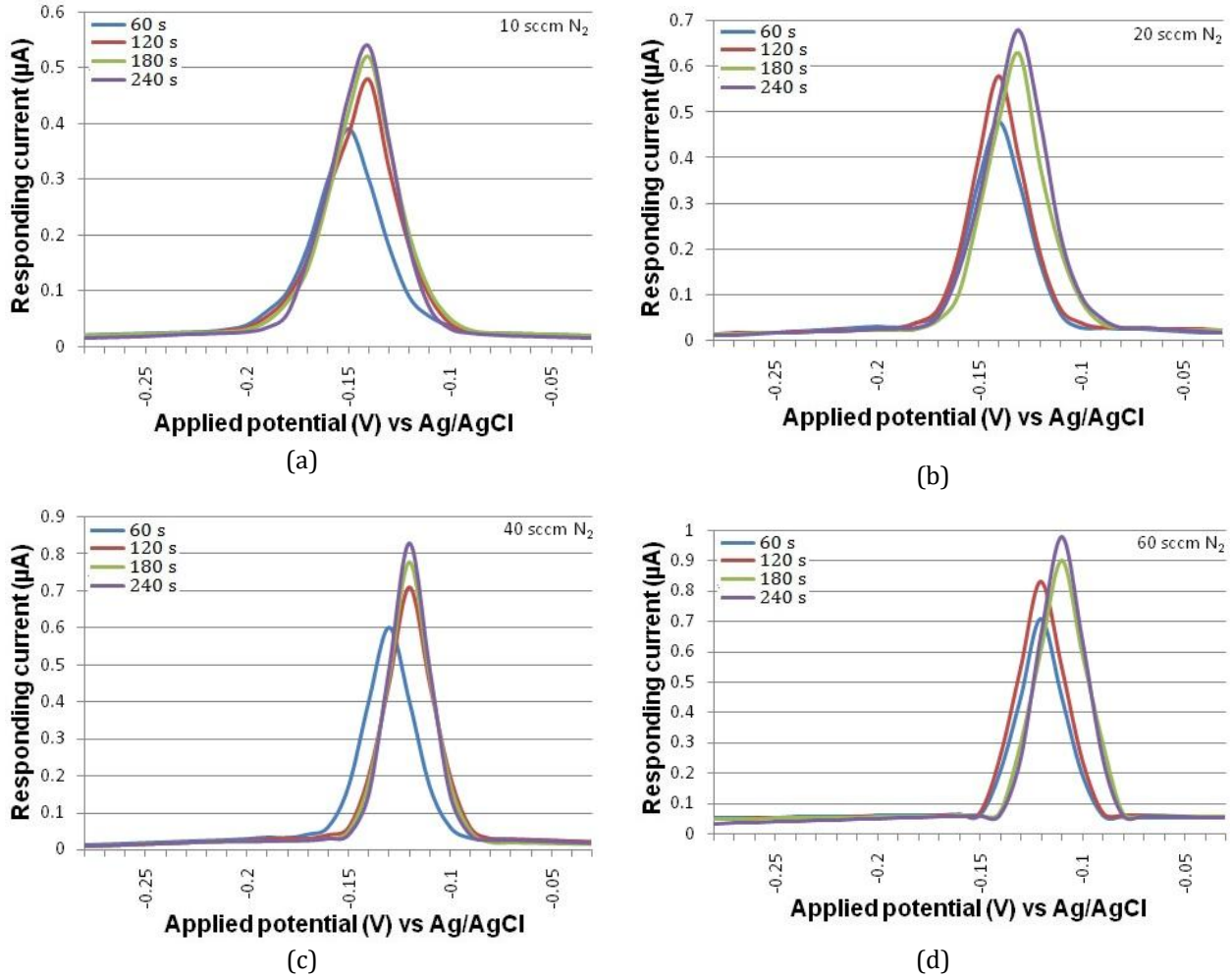

Fig. 3. SWASVs of Cu obtained by N-taC thin films with N_2 flow rates of (a) 10 sccm, (b) 20 sccm, (c) 40 sccm, and (d) 60 sccm in a 1×10^{-6} M Cu^{2+} + 0.1 M KCl solution as a function of deposition time. The deposition potential was -1.2 V.

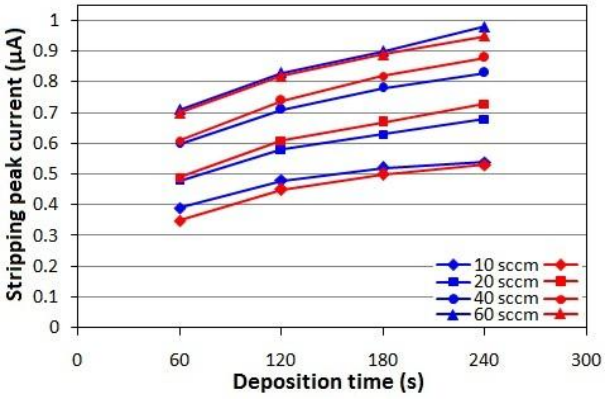

Fig. 4. Stripping peak currents of (red) Pb and (blue) Cu, replotted from SWASVs of Pb and Cu in Figures 2 and 3, respectively, as a function of deposition time.

For both Pb and Cu, the trends of stripping peak current versus deposition time are higher for higher N2 flow rates, which is indicative of the promoted sensitivity of the N-taC thin film to Pb2+ and Cu2+ ions in the KCl solution with its increased N content.

3.3 Effect of deposition potential on SWASVs of Pb and Cu

Figures 5a-d show the SWASVs of Pb obtained by the N-taC thin films with different N_2 flow rates, measured in a 1×10^{-6} M Pb^{2+} + 0.1 M KCl solution for 60 s, as a function of deposition potential. Shifting the deposition potential to more negative values increases the reduction of Pb^{2+} ions on the N-taC thin film surface by accelerating the mobility of Pb^{2+} ions in the pre-concentration step and then gives rise to a proportional increase in the amount of stripped Pb^{2+} ions in the stripping step, resulting in the higher stripping peak intensity of Pb with more negative deposition potential [16,17]. As expected, the stripping peak intensities of Pb deposited at different deposition potentials become higher with higher N_2 flow rates. In Figures 5a-d, the stripping potential of Pb shifts to less negative values by shifting the

deposition potential to more negative values. This can be explained by the higher concentration of stripped Pb^{2+} ions associated with shifting the deposition potential to a more negative value according to the Nernst Equation [9,16-18,31,32]. Herein, the stripping potentials of Pb deposited at different deposition potentials shift to less negative values with higher N_2 flow rates due to the higher concentration of stripped Pb^{2+} ions.

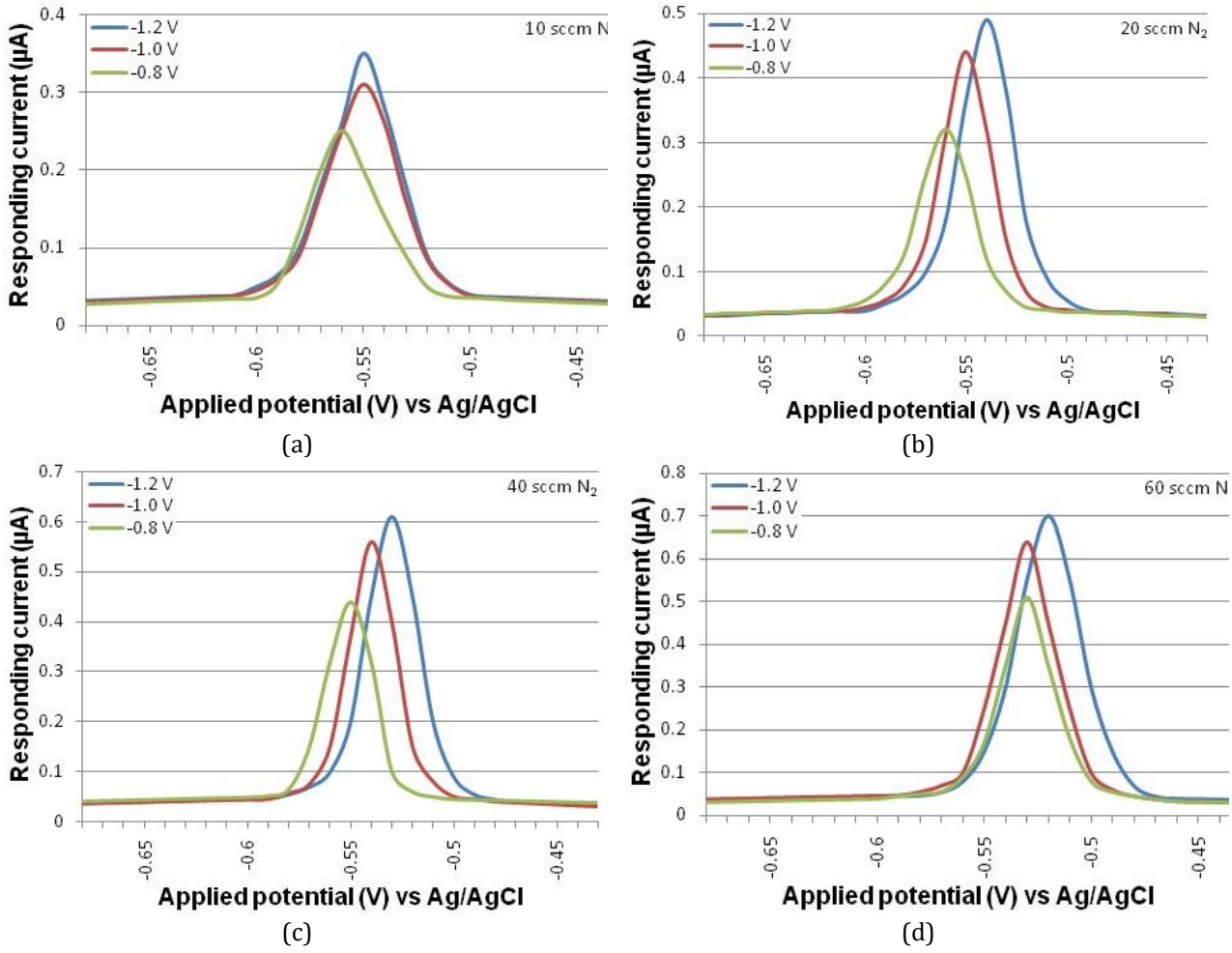

Fig. 5. SWASVs of Pb obtained by N-taC thin films with N_2 flow rates of (a) 10 sccm, (b) 20 sccm, (c) 40 sccm, and (d) 60 sccm in a 1×10^{-6} M Pb^{2+} + 0.1 M KCl solution as a function of deposition potential. The deposition time was 60 s.

Figures 6a-d show the SWASVs of Cu obtained by the N-taC thin films with different N_2 flow rates, measured in a 1×10^{-6} M Cu^{2+} + 0.1 M KCl solution for 60 s, as a function of deposition potential. It is consistently found that the more negative deposition potentials result in the higher stripping peak intensities of Cu for all the N_2 flow rates via the faster mobility of Cu^{2+} ions during accumulation [9,16,18].

The promoted electrical conductivity of the N-taC thin film with an increased N_2 flow rate is responsible for the increased stripping peak intensities of Cu for all the deposition potentials [9,16,18]. In Figures 6a-d, the stripping potentials of Cu consistently shift to less negative values with more negative deposition potentials, as the stripping potentials of Cu obtained at different deposition potentials shift to less negative values with higher N_2 flow rates as a result of the higher concentration of stripped Cu^{2+} ions.

Figures 7a-d show the replotted stripping peak currents of Pb and Cu obtained by the N-taC thin films with different N_2 flow rates as a function of deposition potential. The increased stripping peak currents of both Pb and Cu, with shifting the deposition potential to more negative values are found for all the N_2 flow rates.

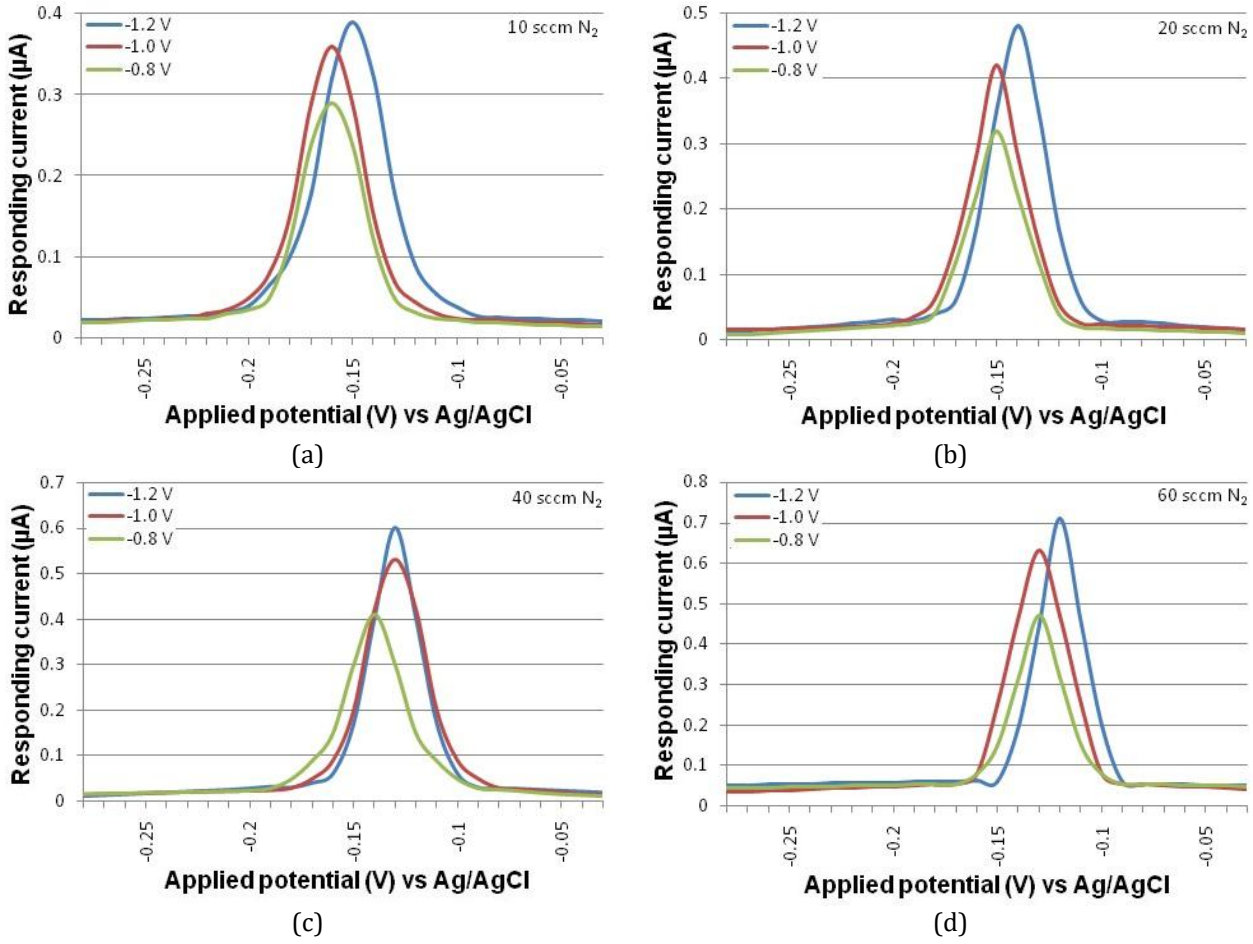

Fig. 6. SWASVs of Cu obtained by N-taC thin films with N_2 flow rates of (a) 10 sccm, (b) 20 sccm, (c) 40 sccm, and (d) 60 sccm in a 1×10^{-6} M Cu^{2+} + 0.1 M KCl solution as a function of deposition potential. The deposition time was 60 s.

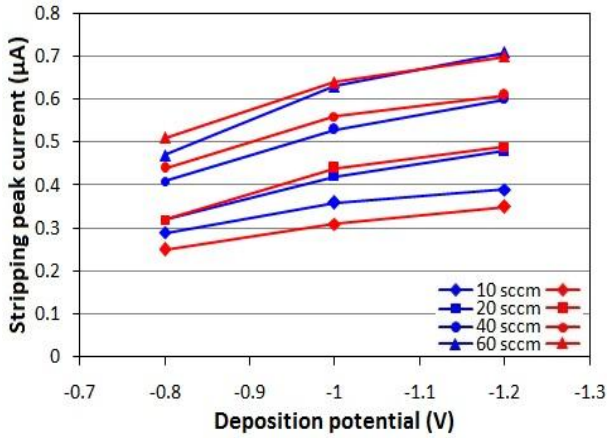

Fig. 7. Stripping peak currents of (red) Pb and (blue) Cu, replotted from SWASVs of Pb and Cu in Figures 5 and 6, as a function of deposition potential, respectively.

The promoted electrical conductivity of the N-taC thin film with a higher N_2 flow rate is responsible for the higher trends of stripping peak current versus deposition potential of both Pb and Cu [9,16,18].

3.4 Effect of metal ion concentration on SWASVs of Pb and Cu

Figures 8a-d show the SWASVs of Pb obtained by the N-taC thin films with different N_2 flow rates, measured in a 0.1 M KCl solution at a deposition potential of -1.2 V for 60 s, as a function of Pb^{2+} ion concentration. It is found that the stripping peak intensities of Pb obtained by the N-taC thin films with different N_2 flow rates become higher with higher Pb^{2+} ion concentrations. Since a high concentration of Pb^{2+} ions in the bulk solution can continuously supply them to the interface by causing and maintaining their great concentration gradient between the surrounding solution and the interface, the higher concentration of Pb^{2+} ions allows for their more reduction on the film surface via their faster transport in the pre-concentration step and thereby their more oxidation in the stripping step for the higher stripping peak intensity of Pb [9,16,18].

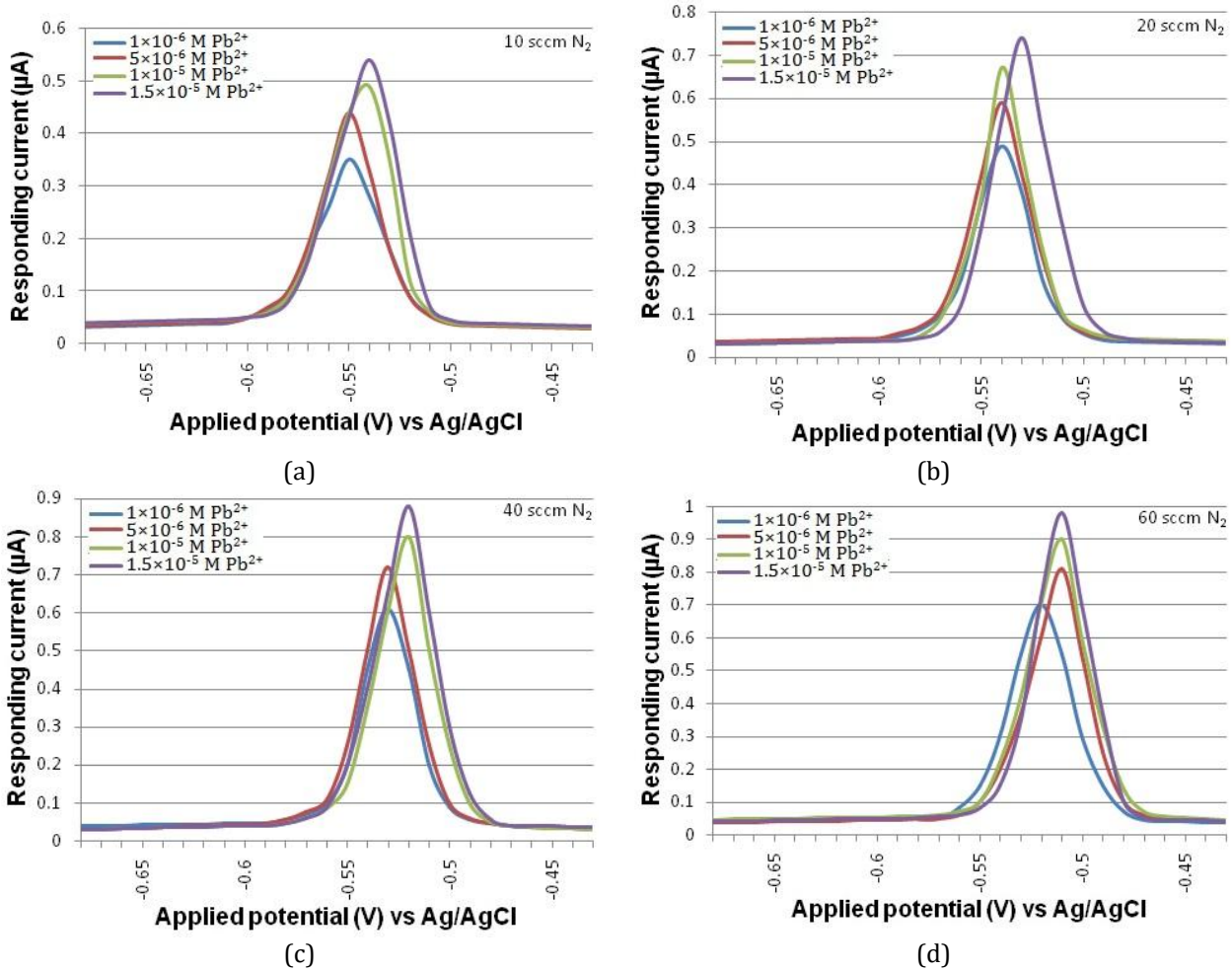

Fig. 8. SWASVs of Pb obtained by N-taC thin films with N_2 flow rates of (a) 10 sccm, (b) 20 sccm, (c) 40 sccm, and (d) 60 sccm in a 0.1 M KCl solution as a function of Pb^{2+} ion concentration. The deposition potential and time were -1.2 V and 60 s, respectively.

For all the Pb^{2+} ion concentrations, the stripping peak intensities of Pb become higher with higher N_2 flow rates due to the promoted electrical conductivity of the N-taC thin film [9,16,18]. As shown in Figures 8a-d, the stripping potentials of Pb shift to less negative values with higher Pb^{2+} ion concentrations or higher N_2 flow rates, which can be correlated to the higher concentration of stripped Pb^{2+} ions according to the Nernst Equation [9,16]. Figures 9a-d show the SWASVs of Cu obtained by the N-taC thin films with different N_2 flow rates, measured in a 0.1 M KCl solution at a deposition potential of -1.2 V for 60 s, as a function of Cu^{2+} ion concentration. As expected, the stripping peak intensities of Cu increase with increased Cu^{2+} ion concentrations or increased N_2 flow rates. A shift of the stripping potentials of Cu to less negative values with higher Cu^{2+} ion concentrations or higher N_2 flow rates is also noticed. This can be explained by applying the Nernst equation since the less negative value of the E associated with the higher concentration of stripped Cu^{2+} ions is responsible for the less negative value of the stripping potential of Cu [9,16].

Figure 10 shows the replotted stripping peak currents of Pb and Cu obtained by the N-taC thin films with different N_2 flow rates as a function of Pb^{2+} and Cu^{2+} ion concentrations, respectively. The N-taC thin films have an increase in the stripping peak currents of Pb and Cu with increased Pb^{2+} and Cu^{2+} ion concentrations, respectively, for all the N_2 flow rates. Increasing the concentration of metal ions in the bulk solution sufficiently supplies them to the interface region as much as they are reduced on the film surface, resulting in a proportional increase in the stripping peak current. The trends of stripping peak current versus metal ion concentration of both Pb and Cu are higher for the higher N_2 flow rates [9,16,18].

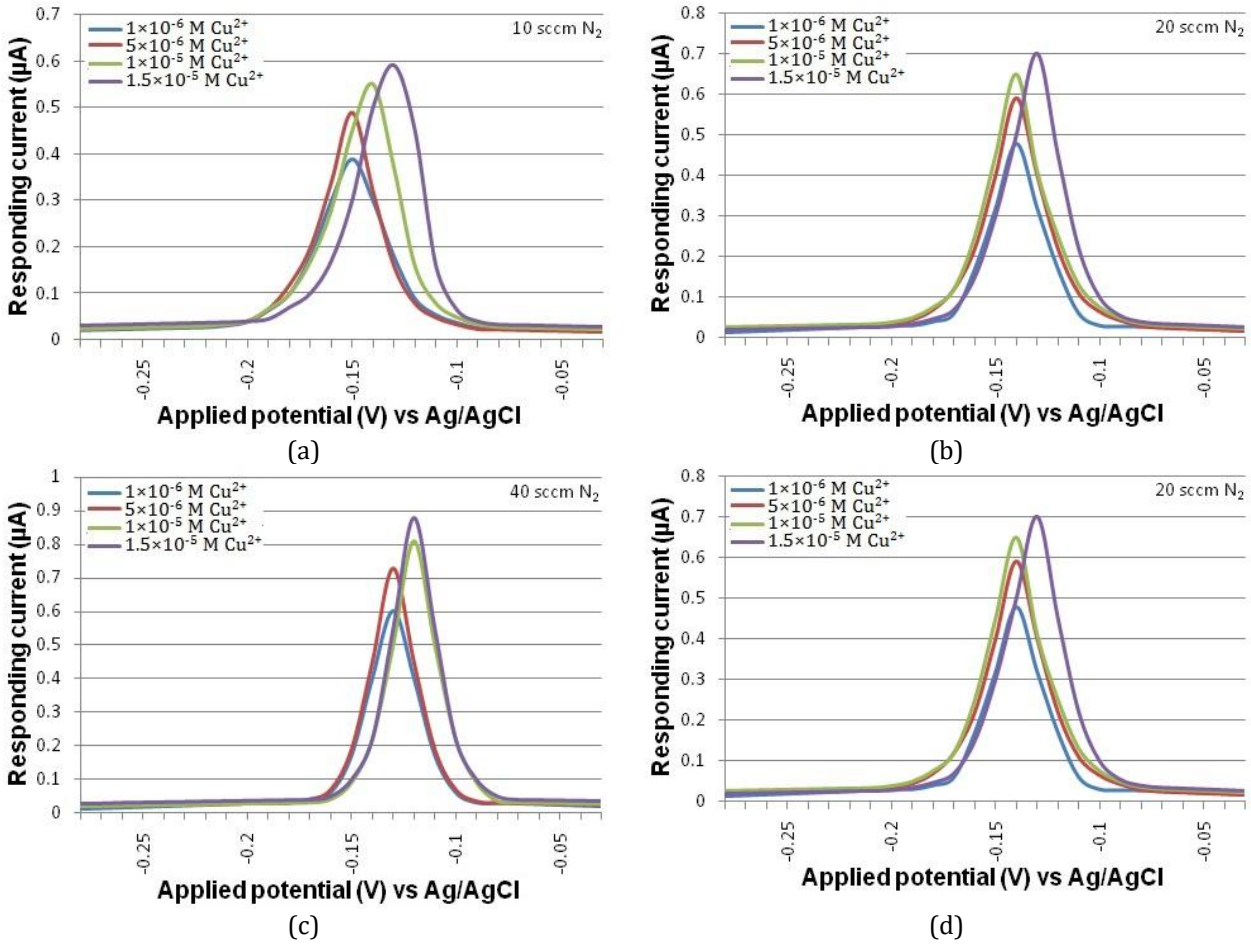

Fig. 9. SWASVs of Cu obtained by N-taC thin films with N_2 flow rates of (a) 10 sccm, (b) 20 sccm, (c) 40 sccm, and (d) 60 sccm in a 0.1 M KCl solution as a function of Cu^{2+} ion concentration. The deposition potential and time were -1.2 V and 60 s, respectively.

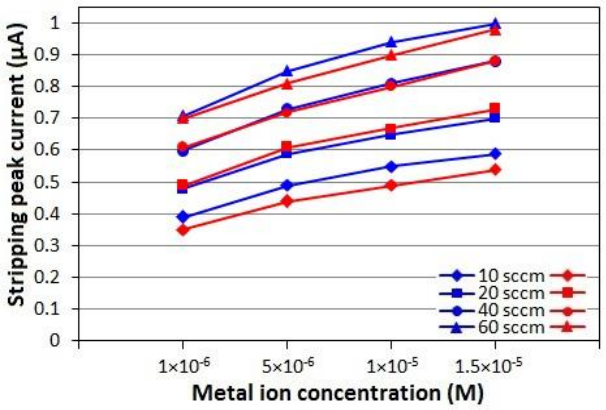

Fig. 10. Stripping peak currents of (red) Pb and (blue) Cu, replotted from SWASVs of Pb and Cu in Figures 8 and 9, as a function of Pb^{2+} and Cu^{2+} ion concentrations, respectively.

4. CONCLUSION

The EPWs of the N-taC thin films with different N_2 flow rates were measured in a 0.1 M KCl solution using the LSCV technique. Then, their SWASV performance was investigated by tracing Pb^{2+} and Cu^{2+} ions in the same solution with respect to deposition time and potential, metal ion concentration, and N_2 flow rate. The following conclusions were drawn.

- The EPW of the N-taC thin film measured in the KCl solution was relatively wide but had an 18.4% decrease from 3.8 V to 3.1 V with an increased N_2 flow rate from 10 to 60 sccm because its lower electrical resistivity associated with its higher N content resulted in the higher kinetics of electron transfer through it and thereby its narrower EPW by causing earlier evolution of H_2 and O_2 gases.
- The stripping peak currents of both Pb and Cu obtained by the N-taC thin films with different N_2 flow rates increased with increased deposition time since the longer deposition time allowed the larger amounts of reduced Pb and Cu atoms on the film

surfaces in the pre-concentration step and, subsequently, the larger amounts of stripped Pb^{2+} and Cu^{2+} ions in the stripping step.

- The stripping peak currents of both Pb and Cu obtained by the N-taC thin films with different N_2 flow rates were higher with more negative deposition potentials because the more negative deposition potential gave rise to the higher mobility of Pb^{2+} and Cu^{2+} ions from the surrounding solution to the interface to reduce them on the film surfaces in the pre-concentration step and thereby the larger amounts of stripped Pb^{2+} and Cu^{2+} ions in the stripping step.
- The stripping peak currents of both Pb and Cu obtained by the N-taC thin films with different N_2 flow rates were higher for the higher concentrations of Pb^{2+} and Cu^{2+} ions because the higher concentrations of Pb^{2+} and Cu^{2+} ions resulted in the larger amounts of reduced Pb and Cu atoms on the film surfaces by causing their greater concentration gradients between the surrounding solution and the interface and hence the larger amounts of stripped Pb^{2+} and Cu^{2+} ions.
- The stripping peak currents of both Pb and Cu increased with increased N_2 flow rate as a result of the promoted electrical conductivity of the N-taC thin film.
- The well-defined SWASVs of Pb and Cu at the μM level clearly indicated that the N-taC thin film had relatively high sensitivity to both Pb^{2+} and Cu^{2+} ions in the aqueous solution.
- It could be concluded that the electrochemical performance of the N-taC thin films was apparently influenced by the deposition time and potential, metal ion concentration, and N content.

Acknowledgment

This work was supported by the research grant (EWI-0601-IRIS-035-00) from the Environment & Water Industry Development Council (EWI), Singapore. The authors would like to thank Dr. Yang Guocheng and Mr. Dinesh Krishna Mohan for their help on this project.

REFERENCES

[1] O. R. Awofolu, Z. Mbolekwa, V. Mtshemla, and O. S. Fatoki, "Levels of trace metals in water and sediment from Tyume river and its effects on irrigated farmland," *Water SA*, vol. 31, no. 1, pp. 87-94, Jul. 2005, doi:10.4314/wsa.v31i1.5124.

[2] T. N. Nguyen, M. Takaoka, T. Kusakabe, and K. Shiota, "Assessing the complexation of dissolved organic matter with heavy metals (Cu^{2+}, Pb^{2+}) in leachate from an old Japanese landfill site using fluorescence quenching," *Environmental Science and Pollution Research*, Aug. 2024, doi:10.1007/s11356-024-34676-x.

[3] Z. Melichova and L. Hromada, "Adsorption of Pb^{2+} and Cu^{2+} ions from aqueous solutions on natural bentonite," *Polish Journal of Environmental Studies*, vol. 22, no. 2, pp. 457-464, Feb. 2023.

[4] M. Subhanullah, N. Hassan, S. Ali, I. A. Saleh, M. Ilya, B. Rawan, W. Ullah, B. Iqbal, M. K. Okla, I. A. Alaraidh, and S. Fahad," *Scientific Reports*, vol. 14, art. no. 2868, Feb. 2024, doi:10.1038/s41598-024-53340-5.

[5] A. L. Wani, A. Ara, and J. A. Usmani, "Lead toxicity: a review," *Interdisciplinary Toxicology*, vol. 8, iss. 2, pp. 55-64, Jun. 2015, doi:10.1515%2Fintox-2015-0009.

[6] L. M. Gaetke, H. S. C. Johnson, and C. K. Chow, "Copper: toxicological relevance and mechanisms," *Archives of Toxicology*, vol. 88, iss. 11, pp. 1929-1938, Nov. 2014, doi:10.1007%2Fs00204-014-1355-y.

[7] M. Radfard, H. Hashemi, M. A. Baghapour, M. R. Samaei, M. Yunesian, H. Soleimani, and A. Azhdarpoor, "Prediction of human health risk and disability-adjusted life years induced by heavy metal exposure through drinking water in Fars Province, Iran," *Scientific Reports*, vol. 13, art. no. 19080, Nov. 2023, doi:10.1038/s41598-023-46262-1.

[8] N. A. A. Qasem, R. H. Mohammed, and D. U. Lawal, "Removal of heavy metal ions from wastewater: a comprehensive and critical review," *npj Clean Water*, vol. 4, art. no. 36, Jul. 2021, doi:10.1038/s41545-021-00127-0.

[9] C. M. A. Brett and A. M. O. Brett, "Electroanalysis," UK, Oxford University Press, 2005.

[10] V. Uskokovic, "A historical review of glassy carbon: synthesis, structure, properties, and applications," *Carbon Trends*, vol. 5, pp. 100116, Oct. 2021, doi:10.1016/j.cartre.2021.100116.

[11] S. Michalkiewicz, A. Skorupa, and M. Jakubczyk, "Carbon materials in electroanalysis of preservatives: a review," *Materials (Basel)*, vol. 14, iss. 24, pp. 7630, Dec. 2021, doi:10.3390%2Fma14247630.

[12] O. E. Tall, N. J. Renault, M. Sigaud, and O. Vittori, “Anodic stripping voltammetry of heavy metals at nanocrystalline boron-doped diamond electrode," *Electroanalysis*, Vol. 19, iss. 11, pp. 1152-1159, Jun. 2007, doi:10.1002/elan.200603834.

[13] S. O. Ganiyu, E. V. D. Santos, C. A. M. Huitle, and S. R. Waldvogel, "Opportunities and challenges of thin film boron-doped diamond electrochemistry for valuable resources' recovery from waste: organic, inorganic, and volatile product electrosynthesis," *Current Opinion in Electrochemistry*, vol. 32, pp. 100903, Apr. 2022, doi:10.1016/j.coelec.2021.100903.

[14] T. Kondo, "Recent electroanalytical applications of boron-doped diamond electrodes," *Current Opinion in Electrochemistry*, vol. 31, pp. 100891, Apr. 2022, doi:10.1016/j.coelec.2021.100891.

[15] K. Yoo, B. Miller, R. Kalish, and X. Shi, "Electrodes of nitrogen-incorporated tetrahedral amorphous carbon: a novel thin-film electrocatalytic material with diamond-like stability," *Electrochemical and Solid-States Letters*, vol. 2, no. 5, pp. 233, Mar. 1999, doi: 10.1149/1.1390794.

[16] N. W. Khun and E. Liu, "Linear sweep anodic stripping voltammetry of heavy metals from nitrogen-doped tetrahedral amorphous carbon thin films," *Electrochimica Acta*, vol. 54, iss. 10, pp. 2890-2898, Apr. 2009, doi:10.1016/j.electacta.2008.11.014.

[17] L. X. Liu and E. Liu, "Nitrogenated diamond-like carbon films for metal tracing," *Surface and Coatings Technology*, vol. 198, iss. 1-3, pp. 189-193, Aug. 2005, doi:10.1016/j.surfcoat.2004.10.031.

[18] X. Shi, H. Fu, J. R. Shi, L. K. Cheah, B. K. Tay, and P. Hui, "Electronic transport properties of nitrogen-doped amorphous carbon films deposited by the filtered cathodic vacuum technique," *Journal of Physics: Condensed Matter*, vol. 10, no. 41, pp. 9293, 1998, doi:10.1088/0953-8984/10/41/011.

[19] N. W. Khun and E. Liu, "Friction and wear of nitrogen-doped DLC coating and platinum/ruthenium/nitrogen co-doped DLC nanocomposite coatings," *Journal of Materials and Engineering*, vol. 3, iss. 1, pp. 67–77, 2025, doi: 10.61552/JME.2025.01.004.

[20] N. W. Khun and E. Liu, "Effect of Ti sputtering power on structures and corrosion resistance of titanium-doped diamond-like carbon nanocomposite thin films," *Journal of Materials and Engineering*, vol. 3, iss. 3, pp. 308-319, 2025, doi:10.61552/JME.2025.03.007.

[21] P. M. Yin, Z. Liu, X. Cao, Z. Lu, and G. Zhang, "Evaluation of the corrosion protection effect of amorphous carbon coating through the corrosion behavior on different substrates," *Diamond and Related Materials*, vol. 142, pp. 110771, Feb. 2024, doi:10.1016/j.diamond.2023.110771.

[22] A. Zeng, E. Liu, S. N. Tan, S. Zhang, and J. Gao, "Stripping voltammetric analysis of heavy metals at nitrogen-doped diamond-like film electrodes," *Electroanalysis*, vol. 14, iss. 18, pp. 1294-1298, Oct. 2002, doi:10.1002/1521-4109(200210)14:18%3C1294::AID-ELAN1294%3E3.0.CO;2-R.

[23] A. Zeng, E. Liu, S. N. Tan, S. Zhang, and J. Gao, "Cyclic voltammetry studies of sputtered nitrogen-doped diamond-like carbon film electrodes," *Electroanalysis*, vol. 14, iss. 15-16, pp. 1110-1115, Aug. 2002,

[24] A. Lagrini, S. Charvet, M. Benlahsen, H. Cachet, and C. Deslouis, "On the relationship between microstructure and electrochemical reactivity of sputtered amorphous carbon nitride electrodes," *Diamond and Related Materials*, vol. 16, iss. 4-7, pp. 1378-1382, Jul. 2007, doi:10.1016/j.diamond.2007.01.006.

[25] N. W. Khun, E. Liu, and H. W. Guo, "Cyclic voltammetric behavior of nitrogen-doped tetrahedral amorphous carbon films deposited by filtered cathodic vacuum arc," *Electroanalysis*, vol. 20, iss. 7, pp. 1851-1856, Sep. 2008, doi:10.1002/elan.200804249.

[26] N. Akita, Y. Konishi, S. Ogura, M. Imamura, Y. H. Hu, and X. Shi, "Comparison of deposition methods for ultra-thin DLC overcoat film for MR head," *Diamond and Related Materials*, vol. 10, iss. 3-7, pp. 1017-1023, Jul. 2001, doi:10.1016/S0925-9635(00)00487-8.

[27] Y. Yi, G. Weinberg, M. Prenzel, M. Greiner, S. Heumann, S. Becker, and R. Schlogl, "Electrochemical corrosion of a glassy carbon electrode," *Catalysis Today*, vol. 295, pp. 32-40, Oct. 2017, doi:10.1016/j.cattod.2017.07.013.

[28] S. Kundoo and S. Kar, "Nitrogen- and boron-doped diamond-like carbon thin films synthesis by electrodeposition from organic liquids and their characterization," *Advances in Materials Physics and Chemistry*, vol. 3, no. 1, pp. 25-32, Mar. 2013, doi:10.4236/ampc.2013.31005.

[29] M. Nilkar, F. E. Ghodsi, S. Jafari, D. Thiry, and R. Snyders, "Effects of nitrogen incorporation on N-doped DLC thin film electrodes fabricated by dielectric barrier discharge plasma: structural evolution and electrochemical performances," *Journal of Alloys and Compounds*, vol. 853, pp. 157298, Feb. 2021, doi:10.1016/j.jallcom.2020.157298.

[30] R. Ferreira, J. Chaar, M. Baldan, and N. Braga, "Simultaneous voltammetric detection of Fe^{3+}, Cu^{2+}, Zn^{2+}, Pb^{2+}, and Cd^{2+} in fuel ethanol using anodic stripping voltammetry and boron-doped diamond electrodes," *Fuel*, vol. 291, pp. 120104, May 2021, doi:10.1016/j.fuel.2020.120104.

[31] G. Gunawardena, G. Hills, and I. Mantenegro, "Electrochemical nucleation: Part IV. Electrodeposition of copper onto vitreous carbon," *Journal of Electroanalytical Chemistry and Interfacial Electrochemistry*, vol. 184, iss. 2, pp. 357-369, Mar. 1985, doi:10.1016/0368-1874(85)85539-8.

[32] M. A. Baldo, C. Bragato, G. A. Mazzocchin, and S. Daniele, "Lead and copper deposition from dilute solutions onto carbon disc microelectrodes. Assessment of qualification procedures by anodic stripping voltammetry," *Electrochimica Acta*, vol. 43, iss. 23, pp. 3413-3422, Jul. 1998, doi:10.1016/S0013-4686(98)00087-5.